Magnetic moment of ^{207}Pb and the hyperfine splitting of ^{207}Pb^{81+}

Verena Fella,[1] Leonid V. Skripnikov,[2,3] Wilfried Nörtershäuser,[4,*] Magnus R. Buchner,[5] H. Lars Deubner,[5] Florian Kraus,[6] Alexei F. Privalov,[1] Vladimir M. Shabaev,[3] and Michael Vogel[1]

[1]*Institut für Festkörperphysik, Technische Universität Darmstadt, Germany*
[2]*B.P. Konstantinov Petersburg Nuclear Physics Institute of National Research Centre "Kurchatov Institute", Gatchina, Leningrad District 188300, Russia*
[3]*Department of Physics, St. Petersburg State University, 198504 St. Petersburg, Russia*
[4]*Institut für Kernphysik, Technische Universität Darmstadt, Germany*
[5]*Institut für Anorganische Chemie, Philipps-Universität Marburg, Germany*
[6]*Fachbereich Chemie, Philipps-Universität Marburg, Germany*

(Received 4 December 2019; accepted 27 February 2020; published 26 March 2020)

We performed nuclear magnetic resonance measurements on lead(II) nitrate $Pb(NO_3)_2$ in aqueous solution and on the hexafluoridoplumbate(IV) $[PbF_6]^{2-}$ ion in acetonitrile. Combined with new relativistic coupled cluster and relativistic density functional theory calculations of the shielding constant, we obtained a magnetic moment of $\mu(^{207}\mathrm{Pb}) = 0.591\,02\,(18)\,\mu_N$ that is in clear disagreement with the tabulated value of $+0.592\,583(9)\,\mu_N$. Similarly as in the case of ^{209}Bi this might be caused by an underestimated chemical shift in the aqueous solution of the nitrate. The consequences for a test of QED in strong magnetic fields by laser spectroscopy of the hyperfine splitting in Pb^{81+} and for the magnetic moments of short-lived lead isotopes are discussed.

DOI: 10.1103/PhysRevResearch.2.013368

I. INTRODUCTION

Nuclear magnetic resonance has been used to determine nuclear magnetic dipole moments for almost 70 years. Besides its ubiquitous use in analytical chemistry, e.g., for decoding molecular structures, it provides nuclear magnetic moments with very high accuracy. Practically all stable and many long-lived isotopes and isomers have been measured with high precision and are tabulated in reference tables like, for example, Ref. [1]. These values are often used as reference values in fundamental and applied physics research. The determination of nuclear moments of short-lived isotopes and isomers from optical hyperfine spectroscopy or β-detected NMR measurements at on-line facilities as tabulated in Ref. [2] is just one example. In this case, NMR reference values of stable or short-lived isotopes are often used to calibrate the externally applied magnetic field or the intrinsic hyperfine fields at the nucleus produced by the electronic shell.

Another example for the importance of nuclear moments in fundamental research is the test of quantum electrodynamics (QED) in extremely strong magnetic fields as they are provided in the vicinity of heavy nuclei. The ground-state hyperfine splitting in hydrogen-like ions has been proposed for such tests and the first heavy ions that have been used in this respect were ^{209}Bi [3] and ^{207}Pb [4] at the experimental storage ring ESR at the GSI Helmholtz Centre for Heavy Ion Research and ^{165}Ho [5], ^{185,187}Re [6], and ^{203,205}Tl [7] at electron beam ion traps. Some of the results showed significant deviations from the QED predictions and it was argued that those arise from the influence of the nuclear moment distribution inside the nucleus called the Bohr-Weisskopf effect. A second line of explanation was that the nuclear moments determined by NMR measurements were inaccurate and a reanalysis of the chemical shifts and NMR frequencies provided in Ref. [8] indicated that some of these values have at least underestimated uncertainties. Recent measurements in hydrogen-like and lithium-like bismuth ions at GSI deviated strongly (7σ) from QED predictions, even though they were combined to a so-called "specific difference" to remove the influence of the Bohr-Weisskopf effect [9]. This triggered new NMR measurements of ^{209}Bi in aqueous $Bi(NO_3)_3$ solutions and on a $[BiF_6]^-$ complex that were combined with relativistic density functional theory and relativistic coupled cluster calculations of the shielding constant and provided a magnetic moment significantly different from the previously accepted value [10]. The new result consistently removed the discrepancies between theoretical predictions and experimental results for the case of the specific difference as well as for the individual transition wavelengths in both charge states $^{209}Bi^{80+,82+}$. Recently, the new value of the magnetic moment has been reconfirmed by NMR on aqueous solutions of $Bi(NO_3)_3$ and $Bi(ClO_4)_3$ salts [11].

For ^{207}Pb the most accurate tabulated value in Ref. [2] of $\mu(^{207}\mathrm{Pb}) = +0.592\,583(9)\,\mu_N$ is also extracted from measurements in aqueous nitrate solutions [12] and has a relative uncertainty similar to the old value of ^{209}Bi, which might as well be underestimated. Moreover, a second value of $0.582\,19(2)\,\mu_N$ was obtained from an optical pumping

*wnoertershaeuser@ikp.tu-darmstadt.de

experiment [13] that strongly disagrees with the NMR value. Since only the NMR value was in agreement with the hyperfine splitting measurement in the hydrogen-like ion [4], it was concluded that the optical pumping result must be erroneous [14]. It turned out that an explanation for the discrepancy between the two values was already given in Ref. [15]: the hyperfine interaction leads to an admixture of the $^3P_1$ state to the $^3P_0$ ground state of the neutral lead atom, which consequently receives some component of the electronic magnetic moment, significantly changing the extracted nuclear magnetic moment. Including the correction lead to a magnetic moment very close to the NMR value [16]. Recent NMR measurements on tetramethyllead $Pb(CH_3)_4$ diluted in gases, lead to a magnetic moment of $\mu(^{207}\mathrm{Pb}) = 0.590\,64(48)\,\mu_\mathrm{N}$ and consistent values, albeit with larger uncertainty, for Pb^{2+} ions in water [17].

For Bi, the most reliable value has been extracted from the NMR of the $[BiF_6]^-$ complex, since it was considerably narrower than the resonance signal from bismuth nitrate solutions and it exhibited only an insignificant temperature dependence whereas the temperature dependence in the aqueous solution was as large as 3 ppm/K [10]. Moreover, the chemical environment was directly proven by the signals septet structure and could be better modelled in the relativistic calculations of the shielding constants than the hydration shell of Bi^{3+}. Therefore, we synthesized the hexafluoridoplumbate(IV) compound $[N(C_2H_5)_4]_2[PbF_6]$, performed NMR measurements in acetonitrile across a temperature range of about 70 K, and compared it to measurements of aqueous lead(II) nitrate solutions in different concentrations and variations in temperature of about 100 K. The results of these measurements are presented in the next section, before we report on the shielding calculations and discuss the conclusions with respect to the hyperfine structure in hydrogen-like $^{207}Pb^{81+}$.

II. EXPERIMENT

A. Sample preparation

1. *General experimental techniques*

All operations were carried out in an atmosphere of dry and purified argon (5.0 Praxair, Germany). Anhydrous HF was dried by mixing it with K_2NiF_6, which reacts with traces of moisture, and separated by vacuum distillation on a Monel Schlenk line. $PbCl_2$ (Merck, p.a.), NaCl (Merck, p.a.), and $[N(C_2H_5)_4]F{\cdot}4H_2O$ (Alfa Aesar, 97%) were used without further purification. Fluorine (Solvay) was passed through a NaF-column to absorb traces of HF and subsequently diluted with argon (5.0 Praxair, Germany) to 10% (V/V) with a flow of 5 ml/min. CD_3CN was dried over P_4O_{10} and distilled prior to use.

2. *Synthesis of* Na_2PbF_6

$PbCl_2$ (837.8 mg, 3.013 mmol) and NaCl (350.7 mg, 6.000 mmol) were mixed by grinding in a mortar. A corundum boat was charged with this mixture and exposed to a stream of diluted fluorine (10% in argon V/V) in a corundum tube furnace at 400 °C (initial heating rate 1 K/min). After three weeks the reaction mixture was transferred into a glovebox, pestled and then reacted for additional four weeks under the conditions given above. Na_2PbF_6 was quantitatively received as a colorless solid.

3. *Synthesis of* $[N(C_2H_5)_4]_2[PbF_6]$

Na_2PbF_6 (270 mg, 0.735 mmol) and $[N(C_2H_5)_4]F{\cdot}4H_2O$ (327 mg, 1.48 mmol) were placed in a FEP Schlenk tube equipped with a stainless steel valve. Anhydrous HF (≈5 ml) was vacuum transferred into the reaction mixture at 196 °C. The reaction vessel was slowly warmed to ambient temperature and subsequently reacted for 3 h under sporadic shaking of the tube. Then the volatiles (HF and H_2O) were carefully removed in vacuo at room temperature to receive the product as a colorless solid.

Samples were prepared by vacuum transferring CD_3CN onto the compounds at −78 °C in an NMR tube which was flame sealed subsequently. The determined NMR spectroscopic data on ^{1}H, ^{13}C, and ^{19}F agreed well with the spectroscopic properties previously described in Ref. [18] (see the Appendix).

B. NMR-Setup for ^{207}Pb Measurements

The NMR measurements were carried out on a 4.9-T BRUKER magnet with a home-built spectrometer controlled by DAMARIS. Further details on the spectrometer components and the software can be found elsewhere [19]. The ^{207}Pb NMR and ^{1}H NMR experiments were performed using the same double resonance probe with a ^{1}H frequency of $\nu_{\mathrm{TMS}} = 200.040445$ MHz and a ^{207}Pb frequency of $\nu_{\mathrm{Pb}} = 41.766707$ MHz to ensure equal conditions for both nuclei. For the ^{1}H NMR calibration tetramethylsilane (TMS) was used as external standard.

Spectra were obtained from the free induction decay following a 90° pulse with a length of 16 μs for ^{207}Pb. Before the signal acquisition a dead time of 4 μs (^{1}H) and 25 μs (^{207}Pb) was implemented as well as a waiting time (1 s for ^{1}H and 4 s to 10 s for ^{207}Pb) between each accumulation to guarantee a full relaxation of the magnetization. The sample temperature was stabilized using a constant gas flow tempered by an electric heater with an accuracy of 1 K.

C. Results

Resonance signals of $^{207}Pb^{2+}$ in aqueous nitrate solutions and $[PbF_6]^{2-}$ in acetonitrile are shown in Figs. 1(a) and 1(b), respectively. For the given chemical shift in ppm tetramethyllead was used as in Ref. [20].

We measured the temperature-dependent resonance frequencies of three different concentrations of aqueous nitrate solutions and of the $[PbF_6]^{2-}$ sample in the temperature range of 255–365 K and 230–300 K, respectively. The results are depicted in Fig. 2. The nitrate solutions exhibit a relatively strong temperature dependence of approximately 1.6 ppm/K, slightly dependent on the concentration, whereas the temperature dependence of the $[PbF_6]^{2-}$ resonance is at least roughly a factor of 30 smaller enabling a more reliable determination of the magnetic moment of ^{207}Pb.

Nuclear magnetic moments can be derived from NMR frequencies ν_r and ν_s if the shielding constants of the reference σ_r and the sample σ_s as well as the magnetic moment μ_r of the

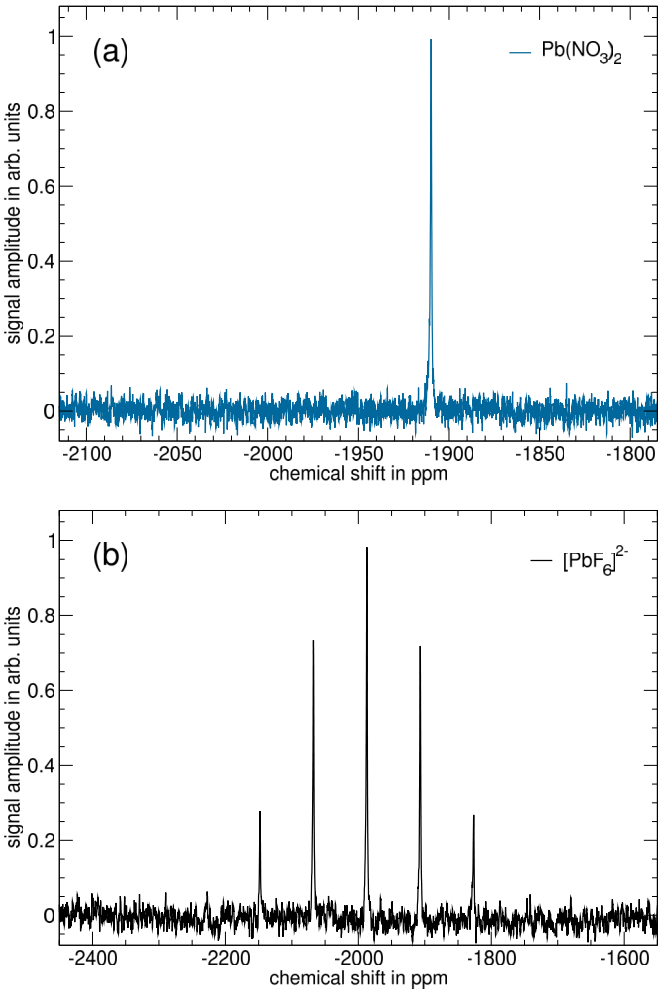

FIG. 1. ^{207}Pb NMR spectra obtained for (a) lead(II) nitrate in an aqueous solution and (b) for hexafluorido-plumbate(IV) ions in acetonitrile. The outermost satellites of the $[PbF_6]^{2-}$-septett are barely visible.

reference are known

$$\mu_s = \frac{\nu_s}{\nu_r}\frac{1-\sigma_r}{1-\sigma_s}\,\mu_r. \tag{1}$$

The shielding constant of $[PbF_6]^{2-}$ was calculated to be 13 393(300) ppm(see Sec. III A) and for TMS the accepted and very small value of 33 ppm [21] was used. Please note that the small temperature and solvent dependence of <1 ppm reported in Ref. [21] can be neglected with respect to our experimental and theoretical uncertainties. The magnetic moment of the bare proton $\mu_p = 2.792\,847\,344\,62(82)\,\mu_N$ was determined recently with high accuracy in a Penning trap applying the continuous Stern-Gerlach effect [22]. With these values we determine the magnetic moment of ^{207}Pb to be

$$\mu(^{207}\mathrm{Pb}) = 0.591\,02\,(18)\,\mu_N. \tag{2}$$

The result is in agreement with the one obtained in Ref. [17] but has about three times smaller uncertainty, being dominated by the uncertainty of the shielding factor. The difference to the tabulated value in Ref. [2] is about eight times the combined uncertainties.

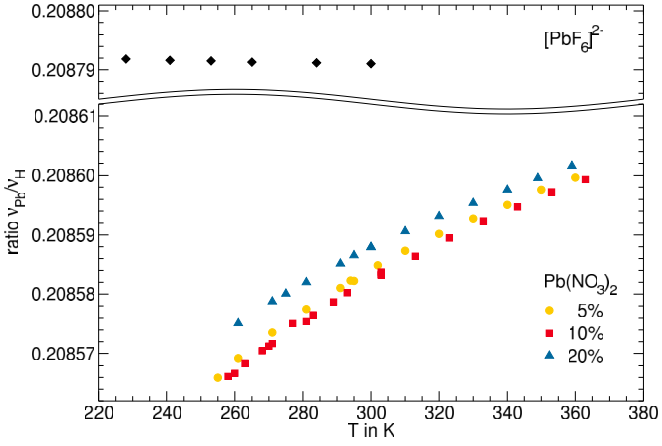

FIG. 2. Temperature dependence of the resonance frequencies for the two sample types. Below the axis break the temperature-dependent frequency ratios ν_{Pb}/ν_H (H in TMS) for aqueous $Pb(NO_3)_2$ solutions are shown for three sample concentrations. The ratio shifts by more than 160 ppm across a temperature range of 100 K. In the case of $[PbF_6]^{2-}$, plotted above the axis break, the shift is less than 5 ppm/80 K.

III. THEORY

A. Shielding calculations

The chemical shielding tensor corresponding to the nucleus j in a molecule can be defined as a mixed derivative of the energy with respect to the nuclear magnetic moment and the strength of the magnetic field B via the following expression:

$$\sigma^j_{a,b} = \left.\frac{\partial^2 E}{\partial\mu_{j,a}\partial B_b}\right|_{\boldsymbol{\mu}_j=0,\mathbf{B}=0}. \tag{3}$$

In the present paper we are interested in the isotropic part of the shielding tensor.

To describe the interaction between electrons in a molecule with an external uniform magnetic field $\mathbf{B}$ one can add the following term to the Dirac-Coulomb Hamiltonian:

$$\mathrm{H}_B = \mathbf{B}\cdot\frac{c}{2}(\boldsymbol{r}_G\times\boldsymbol{\alpha}). \tag{4}$$

Here $\boldsymbol{r}_G = \boldsymbol{r} - \boldsymbol{R}_G$, $\boldsymbol{R}_G$ is the gauge origin and $\boldsymbol{\alpha}$ are the Dirac matrices. The hyperfine interaction of electrons with the magnetic moment $\boldsymbol{\mu}_j$ of the nucleus j is given by the following Hamiltonian:

$$\mathrm{H}_{\mathrm{hyp}} = \frac{1}{c}\sum_j \boldsymbol{\mu}_j\cdot\frac{(\boldsymbol{r}_j\times\boldsymbol{\alpha})}{r_j^3}, \tag{5}$$

where $\boldsymbol{r}_j = \boldsymbol{r} - \boldsymbol{R}_j$, $\boldsymbol{R}_j$ is the position of the nucleus j.

In the one-electron case the shielding tensor (3) can be calculated by the sum-over-states method within the second-order perturbation theory with perturbations (4) and (5). In the relativistic four-component approach the summation should include both positive and negative energy states [23]. The part associated with the former is called "paramagnetic" term while the part associated with the negative energy states is called "diamagnetic term" [23]. Within the many-electron Dirac-Hartree-Fock and density functional theory (DFT)

TABLE I. The values of ^{207}Pb shielding constant contributions in $[PbF_6]^{2-}$ in ppm.

Contribution	Value
Diamagnetic:	
QZQZ-MB-LAO/PBE0	8 492
Paramagnetic:	
QZDZC-RKB/CCSD	4 991
TZDZC-RKB/CCSD(T)-CCSD	−29
Basis set correction	−40
Gaunt	−22
Total	13 393

approaches one can use the response technique to calculate both terms [23–26].

The dependence of the shielding constant value on the choice of the gauge origin $\boldsymbol{R_G}$ can be minimized by using the London atomic orbitals (LAOs) method. It has been formulated and implemented for the four-component DFT methods [25,26].

In relativistic four-component calculations of energy characteristics of free molecules one often uses the restricted kinetic balance (RKB) scheme to obtain the small-component basis set. In the presence of the external magnetic fields the usual relation between the large and small component changes. In Ref. [25] the scheme of the simple magnetic balance (MB) in conjunction with LAOs was proposed to take into account the modified coupling which is utilised below.

The following basis sets were used in shielding constant calculations. The largest used QZQZ basis set corresponds to the uncontracted Dyall's AAE4Z basis set on Pb and Dyall's ACV4Z on F [27,28]. The QZDZC basis set corresponds to the uncontracted AAE4Z basis set on Pb and contracted aug-cc-pVDZ [29,30] on F. In the TZDZC basis set the uncontracted AAE3Z [27,28] basis set is used for Pb and contracted aug-cc-pVDZ [29,30] for F. Finally, we also used the DZDZC basis set which corresponds to uncontracted CVDZ [27,28] basis set on Pb and contracted aug-cc-pVDZ [29,30] on F. Relativistic four-component calculations were performed within the locally modified DIRAC15 [24] and MRCC [31] codes. For calculation of the hyperfine-interaction and *g*-factor matrix elements the code developed in Refs. [32–34] was used. Scalar-relativistic calculations were performed within the USGAMESS [35] and CFOUR [36] codes using the generalized relativistic pseudopotential approach [37,38].

The geometry parameters of the $[PbF_6]^{2-}$ anion were optimized using the four-component coupled cluster method with a correction on the basis set enlargement within the density functional theory with the hybrid Perdew-Burke-Ernzerhof PBE0 functional [39]. We also applied the correction on the solvent effects using the polarizable continuum model and the scalar-relativistic approach. The optimised value of the Pb–F bond length was found to be 2.07 Å.

As was noted previously [10] the paramagnetic part of the shielding tensor strongly depends on the level of the electron correlation effects treatment. Therefore, we used the following scheme to calculate this contribution (see Table I). The leading value was calculated within the relativistic four-component coupled cluster method with single and double amplitudes, CCSD, using the QZDZC basis set. To check the convergence with respect to accounting for electron correlation effects we calculated the contribution of perturbative triple cluster amplitudes within the TZDZC basis set. Also the correction on the basis set enlargement has been calculated as a difference between the values obtained within the QZQZ and QZDZC basis sets using the four-component PBE0 theory [39]. Finally, the contribution of the Gaunt interaction to the shielding constant was estimated as the difference between the values calculated at the Dirac-Hartree-Fock-Gaunt and Dirac-Hartree-Fock levels.

The diamagnetic part of the shielding constant has been calculated within the four-component DFT using the PBE0 functional. Note that in case of the diamagnetic contribution the values calculated within the Dirac-Hartree-Fock and PBE0 theories coincide within a few ppm. However, the values of the *paramagnetic* contribution obtained within these theories differ by more than 1300 ppm. It turns out that the value of the contribution depends strongly on the choice of the functional. For example, we obtained that the application of the PBE [40] and PBE0 [39] functionals leads to the values that differ by more than 700 ppm. The value obtained within the LDA [41] functional differs again by more than 1000 ppm from the PBE0 [39] result. These results provide an uncertainty estimate for DFT-based calculations of the paramagnetic term and indicate that these are not sufficiently accurate for our needs. Instead, in the present paper the paramagnetic term has been calculated within the *ab initio* relativistic coupled cluster theory. In this approach it is possible to directly estimate the uncertainty concerned with the electron correlation effects treatment. For example, within a given basis set we obtained that the inclusion of triple cluster amplitudes changes the value of the paramagnetic term obtained within the coupled cluster with single and double amplitudes by only −29 ppm. This is more than an order of magnitude smaller than the uncertainty of the DFT treatment of the paramagnetic contribution.

Table I gives the final value of the shielding constant as well as its contributions described above. It can be seen that both basis set and correlation corrections on triple cluster amplitudes are rather small. However, some uncertainty can come from the effect of the solvent. To estimate a possible contribution of this effect we calculated the shielding constant for several values of the Pb–F distances and found approximately linear dependence of the shielding constant value on the distance for small distortions. For example, increasing the Pb–F distances by 0.02 Å leads to an increase of the paramagnetic part of the shielding constant value by about 81 ppm [within the relativistic CCSD(T) approach using the DZDZC basis set]. This value can serve as some indirect estimation of the solvent effects. As a direct treatment of these effects is hardly possible at the considered level of theory we conservatively estimate the uncertainty of the final value of the shielding constant as about 300 ppm.

B. Hyperfine structure in Pb^{81+}

The ground-state hyperfine splitting in a H-like ion can be written as

$$\Delta E_{\rm HFS} = \Delta E^{\rm D}_{\rm HFS}(1-\epsilon) + \Delta E^{\rm QED}_{\rm HFS}, \qquad (6)$$

where $\Delta E_{\mathrm{HFS}}^{\mathrm{D}}$ is the Dirac value which incorporates the relativistic and nuclear-charge-distribution effects, $\Delta E_{\mathrm{HFS}}^{\mathrm{QED}}$ is the QED correction, and ϵ takes into account the nuclear-magnetization distribution correction (the so-called Bohr-Weisskopf effect). The calculation of the Dirac value causes no problem. For the nuclear magnetic moment determined in this work, we obtain $\Delta E_{\mathrm{HFS}}^{\mathrm{D}} = 1.2721(4)$ eV. The QED correction was also evaluated by different groups [42–44], yielding $\Delta E_{\mathrm{HFS}}^{\mathrm{QED}} = -0.0073$ eV. Most problematic is the evaluation of the Bohr-Weisskopf correction, which requires using a microscopic nuclear model. The correction is rather sensitive to the choice of the model and generally yields an uncertainty that is of the same order of magnitude as the QED contribution. In the case of ^{207}Pb the nuclear single-particle model predicts the value of the nuclear magnetic moment within 10% of the observed value. This was taken into account in Ref. [14] and it was assumed that the relative uncertainty of the Bohr-Weisskopf correction, calculated within this model, should be approximately the same. The result $\epsilon = 0.042(4)$ reduces the HFS value by $-0.053(5)$ eV and yields a total theoretical value of 1.212(5) eV. A more elaborated evaluation [45], based on the Migdal theory of finite Fermi systems, yielded $\epsilon = 0.0353(-35, +164)$. With the new value of the magnetic moment reported here, this leads to $\Delta E_{\mathrm{HFS}}^{\mathrm{theor}} = 1.220(-21, +4)$ eV. Both theoretical values are in good agreement with the experimental result of $\Delta E_{\mathrm{HFS}}^{\mathrm{exp}} = 1.2159(2)$ eV [4].

IV. CONCLUSION

We performed nuclear magnetic resonance studies of ^{207}Pb in $[PbF_6]^{2-}$ anions and demonstrated that the magnetic moment of ^{207}Pb can be reliably extracted from these measurements in combination with improved relativistic coupled cluster and relativistic density functional theory calculations of the shielding constant. Similar as in the case of Bi [10], the new value differs significantly from the tabulated value $[\approx 8(\sigma_{\mathrm{new}} + \sigma_{\mathrm{old}})]$, which affects the calculation of the hyperfine splitting in highly charged ions. Applying the new value of $\mu(^{207}\mathrm{Pb})$ in these calculations provides good agreement with the previously measured hyperfine splitting in hydrogen-like Pb^{81+} at the GSI Helmholtz Centre for Heavy Ion Research [4].

Please note that ^{207}Pb is also the reference isotope for all studies of magnetic moments of short-lived isotopes. As such, the change also affects their tabulated values. Even though the accuracy of the hyperfine measurements on short-lived lead atoms limits the accuracy of all tabulated magnetic moment values, for ^{203,205,211}Pb the shift is larger than 3σ of the stated uncertainties in Ref. [2]. However, it should be kept in mind that the tabulated uncertainty does also not include the (unknown) hyperfine structure anomaly, which still has to be added to both uncertainties.

In summary, our study substantiates again the fact that magnetic moments provided in literature and review tables have to be taken with care. Future high precision measurements on bare nuclei as they are possible in Penning traps and have been realized already in measuring the magnetic moment of the proton [22] and the antiproton could provide magnetic moments without the need for any diamagnetic shielding corrections. Bare and hydrogen-like ions of heavy elements will be delivered by the HITRAP setup at GSI [46] and the ARTEMIS experiment is designed to perform high-precision measurements of nuclear moments on hydrogen-like or lithium-like systems [47], which are much better understood theoretically than systems with a large number of electrons.

ACKNOWLEDGMENTS

Calculations of the shielding constant were carried out using resources of the collective usage center "Modeling and predicting properties of materials at NRC" "Kurchatov Institute"–PNPI. The performance of the shielding constant calculations were funded solely by the Russian Science Foundation Grant No. 19-72-10019. For the remaining theoretical part V.M.S. and L.V.S. acknowledge the support of the Foundation for the Advancement of Theoretical Physics and Mathematics BASIS. The experimental part was supported by the Federal Ministry of Education and Research of Germany under Contract No. 05P19RDFAA and the Helmholtz International Center for FAIR (HIC for FAIR). We thank C. Geppert from the Institute of Nuclear Chemistry at the University of Mainz for providing the aqueous NMR samples.

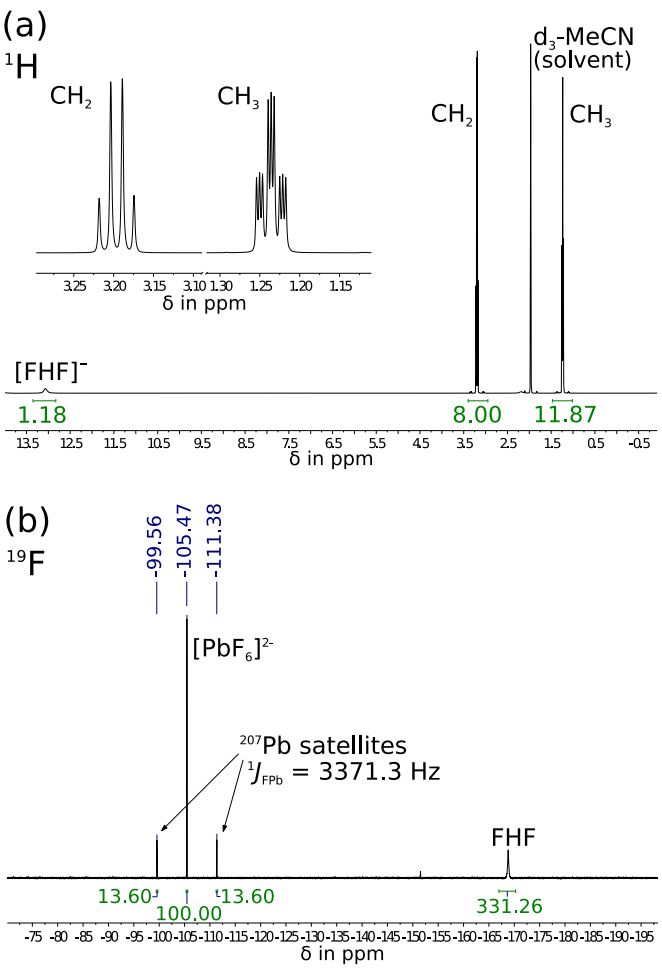

FIG. 3. NMR spectra obtained for $[N(C_2H_5)_4]_2[PbF_6]$ in acetonitrile with (a) ^{1}H NMR and (b) ^{19}F NMR after synthesis.

APPENDIX: SAMPLE CHARACTERIZATION

^{1}H and ^{13}C NMR spectra were recorded on a Bruker Avance III 500 spectrometer equipped with a Prodigy CryoProbe. ^{1}H NMR (500 MHz) and ^{13}C NMR (126 MHz) chemical shifts are given relative to the solvent signal for CD_3CN (1.94 and 1.32 ppm). ^{19}F NMR (282 MHz) spectra were recorded on a Bruker Avance III HD 300 spectrometer and used $CFCl_3$ (0 ppm) as an external standard. NMR spectra were processed with the MestReNova software.

The resulting ^{1}H and ^{19}F NMR spectra for $[N(C_2H_5)_4]_2[PbF_6]$ are shown in Fig. 3 and yielded the following spectroscopic properties.

^{1}H NMR (500 MHz, 300 K, CD_3CN)

$\delta = 1.21$ (tt, $^{3}J_{HH} = 7.3$ Hz, $^{3}J_{NH} = 1.9$ Hz, 12H; CH_3), 3.17 ppm (q, $^{3}J_{HH} = 7.3$ Hz, 8H, CH_2).

^{13}C{^{1}H} NMR (126 MHz, 300 K, CD_3CN)

$\delta = 7.6$ (s, CH_3), 53.0 ppm (t, $^{1}J_{NC} = 3.2$ Hz, CH_2).

^{19}F{^{1}H} NMR (282 MHz, 300 K, CD_3CN)

$\delta = 105.47$ ppm (s, $^{1}J_{PbF} = 3371.3$ Hz).

This is in good agreement with NMR spectroscopic properties previously described in Ref. [18]: ^{19}F{^{1}H} NMR (471 MHz, 306 K, CD_3CN) $\delta = 103.8$ ppm (s, $^{1}J_{PbF} = 3331$ Hz).

[1] E. Cohen, T. Cvitas, J. Frey, B. Holmstrom, K. Kuchitsu, R. Marquardt, I. Mills, F. Pavese, M. Quack, J. Stohner, H. Strauss, M. Takami, and A. Thor, *Quantities, Units and Symbols in Physical Chemistry, IUPAC Green Book* (Blackwell Science, Hoboken, NJ, 2007).

[2] N. Stone, Table of nuclear magnetic dipole and electric quadrupole moments, INDC(NDS)–0658, International Atomic Energy Agency (IAEA) (2014).

[3] I. Klaft, S. Borneis, T. Engel, B. Fricke, R. Grieser, G. Huber, T. Kühl, D. Marx, R. Neumann, S. Schröder, P. Seelig, and L. Völker, Precision Laser Spectroscopy of the Ground State Hyperfine Splitting of Hydrogenlike $^{209}Bi^{82+}$, Phys. Rev. Lett. **73**, 2425 (1994).

[4] P. Seelig, S. Borneis, A. Dax, T. Engel, S. Faber, M. Gerlach, C. Holbrow, G. Huber, T. Kühl, D. Marx, K. Meier, P. Merz, W. Quint, F. Schmitt, M. Tomaselli, L. Völker, H. Winter, M. Würtz, K. Beckert, B. Franzke, F. Nolden, H. Reich, M. Steck, and T. Winkler, Ground State Hyperfine Splitting of Hydrogenlike $^{207}Pb^{81+}$ by Laser Excitation of a Bunched Ion Beam in the GSI Experimental Storage Ring, Phys. Rev. Lett. **81**, 4824 (1998).

[5] J. R. Crespo López-Urrutia, P. Beiersdorfer, D. W. Savin, and K. Widmann, Direct Observation of the Spontaneous Emission of the Hyperfine Transition F = 4 to F = 3 in Ground State Hydrogenlike $^{165}Ho^{66+}$ in an Electron Beam Ion Trap, Phys. Rev. Lett. **77**, 826 (1996).

[6] J. R. C. Crespo López-Urrutia, P. Beiersdorfer, K. Widmann, B. B. Birkett, A.-M. Martensson-Pendrill, and M. G. H. Gustavsson, Nuclear magnetization distribution radii determined by hyperfine transitions in the 1s level of H-like ions $^{185}Re^{74+}$ and $^{187}Re^{74+}$, Phys. Rev. A **57**, 879 (1998).

[7] P. Beiersdorfer, S. B. Utter, K. L. Wong, J. R. Crespo López-Urrutia, J. A. Britten, H. Chen, C. L. Harris, R. S. Thoe, D. B. Thorn, E. Träbert, M. G. H. Gustavsson, C. Forssén, and A.-M. Mårtensson-Pendrill, Hyperfine structure of hydrogenlike thallium isotopes, Phys. Rev. A **64**, 032506 (2001).

[8] M. G. H. Gustavsson and A.-M. Mårtensson-Pendrill, Need for remeasurements of nuclear magnetic dipole moments, Phys. Rev. A **58**, 3611 (1998).

[9] J. Ullmann, Z. Andelkovic, C. Brandau, A. Dax, W. Geithner, C. Geppert, C. Gorges, M. Hammen, V. Hannen, S. Kaufmann, K. König, Y. Litvinov, M. Lochmann, B. Maas, J. Meisner, T. Murböck, R. Sánchez, M. Schmidt, S. Schmidt, M. Steck, T. Stöhlker, R. Thompson, C. Trageser, J. Vollbrecht, C. Weinheimer, and W. Nörtershäuser, High precision hyperfine measurements in bismuth challenge bound-state strong-field QED, Nat. Commun. **8**, 15484 (2017).

[10] L. V. Skripnikov, S. Schmidt, J. Ullmann, C. Geppert, F. Kraus, B. Kresse, W. Nörtershäuser, A. F. Privalov, B. Scheibe, V. M. Shabaev, M. Vogel, and A. V. Volotka, New Nuclear Magnetic Moment of ^{209}Bi: Resolving the Bismuth Hyperfine Puzzle, Phys. Rev. Lett. **120**, 093001 (2018).

[11] A. Antušek, M. Repisky, M. Jaszuński, K. Jackowski, W. Makulski, and M. Misiak, Nuclear magnetic dipole moment of ^{209}Bi from NMR experiments, Phys. Rev. A **98**, 052509 (2018).

[12] O. Lutz and G. Stricker, The magnetic moment of ^{207}Pb and the shielding of lead ions by water, Phys. Lett. A **35**, 397 (1971).

[13] H. M. Gibbs and C. M. White, Polarization of Pb vapor. II. Disorientation of the Pb^{207} ground state and $\mu_I(Pb^{207})/\mu_I(Hg^{199})$, Phys. Rev. **188**, 180 (1969).

[14] V. Shabaev, M. Shabaeva, I. Tupitsyn, and V. Yerokhin, Hyperfine structure of highly charged ions, Hyperf. Int. **114**, 129 (1998).

[15] O. P. Sushkov, V. V. Flambaum, and I. B. Khriplovich, Theory of hyperfine structure of heavy atoms, Opt. Spectr. (USSR) **44**, 3 (1978).

[16] V. Shabaev, A. Artemyev, O. Zherebtsov, V. Yerokhin, G. Plunien, and G. Soff, Calculation of the hyperfine structure of heavy H and Li like ions, Hyperf. Int. **127**, 279 (2000).

[17] B. Adrjan, W. Makulski, K. Jackowski, T. B. Demissie, K. Ruud, A. Antušek, and M. Jaszuński, NMR absolute shielding scale and nuclear magnetic dipole moment of ^{207}Pb, Phys. Chem. Chem. Phys. **18**, 16483 (2016).

[18] D. Hutchison, J. Sanders, and G. Schrobilgen, Synthesis and characterization by ^{19}F and ^{207}Pb NMR spectroscopy of the $[PbCl_nF_{6-n}]^{2-}$ anions (n=0-6), Eur. J. Solid State Inorg. Chem. **33**, 795 (1996).

[19] A. Gädke, M. Rosenstihl, C. Schmitt, H. Stork, and N. Nestle, DAMARIS–a flexible and open software platform for NMR spectrometer control, Diffusion Fundamentals **5**, 1 (2007).

[20] R. K. Harris, E. D. Becker, S. M. C. De Menezes, R. Goodfellow, and P. Granger, NMR nomenclature. Nuclear spin properties and conventions for chemical shifts (IUPAC recommendations 2001), Pure Appl. Chem. **73**, 1795 (2001).

[21] P. Garbacz and K. Jackowski, Referencing of ^{1}H and ^{13}C NMR shielding measurements, Chem. Phys. Lett. **728**, 148 (2019).

[22] G. Schneider, A. Mooser, M. Bohman, N. Schön, J. Harrington, T. Higuchi, H. Nagahama, S. Sellner, C. Smorra, K. Blaum, Y. Matsuda, W. Quint, J. Walz, and S. Ulmer, Double-trap measurement of the proton magnetic moment at 0.3 parts per billion precision, Science **358**, 1081 (2017).

[23] G. A. Aucar, T. Saue, L. Visscher, and H. J. A. Jensen, On the origin and contribution of the diamagnetic term in four-component relativistic calculations of magnetic properties, J. Chem. Phys. **110**, 6208 (1999).

[24] DIRAC, a relativistic *ab initio* electronic structure program, Release DIRAC15 (2015), written by R. Bast, T. Saue, L. Visscher, and H. J. Aa. Jensen, with contributions from V. Bakken, K. G. Dyall, S. Dubillard, U. Ekstroem, E. Eliav, T. Enevoldsen, E. Fasshauer, T. Fleig, O. Fossgaard, A. S. P. Gomes, T. Helgaker, J. Henriksson, M. Ilias, Ch. R. Jacob, S. Knecht, S. Komorovsky, O. Kullie, J. K. Laerdahl, C. V. Larsen, Y. S. Lee, H. S. Nataraj, M. K. Nayak, P. Norman, G. Olejniczak, J. Olsen, Y. C. Park, J. K. Pedersen, M. Pernpointner, R. Di Remigio, K. Ruud, P. Salek, B. Schimmelpfennig, J. Sikkema, A. J. Thorvaldsen, J. Thyssen, J. van Stralen, S. Villaume, O. Visser, T. Winther, and S. Yamamoto (see http://www.diracprogram.org).

[25] M. Olejniczak, R. Bast, T. Saue, and M. Pecul, A simple scheme for magnetic balance in four-component relativistic Kohn-Sham calculations of nuclear magnetic resonance shielding constants in a Gaussian basis, J. Chem. Phys. **136**, 014108 (2012).

[26] M. Ilias, H. J. A. Jensen, R. Bast, and T. Saue, Gauge origin independent calculations of molecular magnetisabilities in relativistic four-component theory, Mol. Phys. **111**, 1373 (2013).

[27] K. G. Dyall, Relativistic double-zeta, triple-zeta, and quadruple-zeta basis sets for the actinides Ac–Lr, Theor. Chem. Acc. **117**, 491 (2007).

[28] K. G. Dyall, Core correlating basis functions for elements 31–118, Theor. Chem. Acc. **131**, 1217 (2012).

[29] T. H. Dunning, Jr., Gaussian basis sets for use in correlated molecular calculations. I. The atoms boron through neon and hydrogen, J. Chem. Phys. **90**, 1007 (1989).

[30] R. A. Kendall, T. H. Dunning, Jr., and R. J. Harrison, Electron affinities of the first-row atoms revisited. Systematic basis sets and wave functions, J. Chem. Phys. **96**, 6796 (1992).

[31] M. Kállay, P. R. Nagy, D. Mester, Z. Rolik, G. Samu, J. Csontos, J. Csóka, P. B. Szabó, L. Gyevi-Nagy, B. Hégely, I. Ladjánszki, L. Szegedy, B. Ladóczki, K. Petrov, M. Farkas, P. D. Mezei, and Á. Ganyecz, The MRCC program system: Accurate quantum chemistry from water to proteins, J. Chem. Phys. **152**, 074107 (2020). MRCC, a quantum chemical program suite written by M. Kállay, P. R. Nagy, D. Mester, Z. Rolik, G. Samu, J. Csontos, J. Csóka, P. B. Szabó, L. Gyevi-Nagy, B. Hégely, I. Ladjánszki, L. Szegedy, B. Ladóczki, K. Petrov, M. Farkas, P. D. Mezei, and Á. Ganyecz, see www.mrcc.hu.

[32] L. V. Skripnikov, Combined 4-component and relativistic pseudopotential study of ThO for the electron electric dipole moment search, J. Chem. Phys. **145**, 214301 (2016).

[33] L. V. Skripnikov and A. V. Titov, Theoretical study of ThF^+ in the search for T, P-violation effects: Effective state of a Th atom in ThF^+ and ThO compounds, Phys. Rev. A **91**, 042504 (2015).

[34] L. V. Skripnikov and A. V. Titov, Theoretical study of thorium monoxide for the electron electric dipole moment search: Electronic properties of $H^3\Delta_1$ in ThO, J. Chem. Phys. **142**, 024301 (2015).

[35] M. W. Schmidt, K. K. Baldridge, J. A. Boatz, S. T. Elbert, M. S. Gordon, J. H. Jensen, S. Koseki, N. Matsunaga, K. A. Nguyen, S. J. Su, T. L. Windus, M. Dupuis, and J. A. Montgomery, General atomic and molecular electronic structure system, J. Comput. Chem. **14**, 1347 (1993).

[36] J. F. Stanton *et al.*, "CFOUR" (2011), CFOUR: a program package for performing high-level quantum chemical calculations on atoms and molecules, http://www.cfour.de.

[37] N. S. Mosyagin, A. V. Zaitsevskii, L. V. Skripnikov, and A. V. Titov, Generalized relativistic effective core potentials for actinides, Int. J. Quantum Chem. **116**, 301 (2016).

[38] L. V. Skripnikov, A. D. Kudashov, A. N. Petrov, and A. V. Titov, Search for parity- and time-and-parity–violation effects in lead monofluoride (PbF): *Ab initio* molecular study, Phys. Rev. A **90**, 064501 (2014).

[39] C. Adamo and V. Barone, Toward reliable density functional methods without adjustable parameters: The PBE0 model, J. Chem. Phys. **110**, 6158 (1999).

[40] J. P. Perdew, K. Burke, and M. Ernzerhof, Generalized Gradient Approximation Made Simple, Phys. Rev. Lett. **77**, 3865 (1996).

[41] S. H. Vosko, L. Wilk, and M. Nusair, Accurate spin-dependent electron liquid correlation energies for local spin density calculations: a critical analysis, Canad. J. Phys. **58**, 1200 (1980).

[42] V. M. Shabaev, M. Tomaselli, T. Kühl, A. N. Artemyev, and V. A. Yerokhin, Ground-state hyperfine splitting of high-Z hydrogenlike ions, Phys. Rev. A **56**, 252 (1997).

[43] P. Sunnergren, H. Persson, S. Salomonson, S. M. Schneider, I. Lindgren, and G. Soff, Radiative corrections to the hyperfine-structure splitting of hydrogenlike systems, Phys. Rev. A **58**, 1055 (1998).

[44] A. N. Artemyev, V. M. Shabaev, G. Plunien, G. Soff, and V. A. Yerokhin, Vacuum-polarization corrections to the hyperfine splitting in heavy ions and to the nuclear magnetic moments, Phys. Rev. A **63**, 062504 (2001).

[45] R. Sen'kov and V. Dmitriev, Nuclear magnetization distribution and hyperfine splitting in Bi^{82+} ion, Nucl. Phys. A **706**, 351 (2002).

[46] H.-J. Kluge, T. Beier, K. Blaum, L. Dahl, S. Eliseev, F. Herfurth, B. Hofmann, O. Kester, S. Koszudowski, C. Kozhuharov, G. Maero, W. Nörtershäuser, J. Pfister, W. Quint, U. Ratzinger, A. Schempp, R. Schuch, T. Stöhlker, R. Thompson, M. Vogel, G. Vorobjev, D. Winters, and G. Werth, HITRAP: A facility at GSI for highly charged ions, Adv. Quant. Chem. **53**, 83 (2008).

[47] W. Quint, D. L. Moskovkhin, V. M. Shabaev, and M. Vogel, Laser-microwave double-resonance technique for g-factor measurements in highly charged ions, Phys. Rev. A **78**, 032517 (2008).